SDSS'Rio 2010 STABILITY AND DUCTILITY OF STEEL STRUCTURES
E. Batista, P. Vellasco, L. de Lima (Eds.)
Rio de Janeiro, Brazil, September 8 - 10, 2010

INFLUENCE OF HOLES ON THE BEHAVIOUR OF COLD-FORMED STEEL SECTIONS UNDER COMPRESSION

M.M. Pastor, M. Casafont, F. Roure, J. Bonada and J. Noguera

Department of Strength of Materials and Structural Engineering
Escola Tècnica Superior d'Enginyeria Industrial de Barcelona (ETSEIB)
Universitat Politècnica de Catalunya (UPC)
Av. Diagonal, 647, 08028 Barcelona
m.magdalena.pastor@upc.edu, miquel.casafont@upc.edu, francesc.roure@upc.edu

Keywords: Rack, Upright, Stability, Perforations.

Abstract. *The uprights in a pallet-rack system are mono-symmetrical open cold-formed thin-walled steel sections, with slots and holes along their length. The perforations are needed for connecting the beams and the diagonals to the uprights. Due to their slenderness, the usual mode of failure of these members is buckling. Depending on the member length, the form of buckling is (basically) local, distortional or global. There are different ways of determining the actual strength of the uprights under compression: experimental, analytical and numerical. In some of the analytical and numerical methods, the effect of the perforations is taken into account by using an "effective thickness" of the section (instead of the true thickness). The aim of this paper is to establish a means of determining this "effective thickness", based on the experimental tests performed on the same upright, with and without perforations. Analyses by FE simulation are carried out on the same upright, with perforations, without perforations and real thickness, and without perforations and "effective thickness"; and, finally, the "effective thickness" is adjusted to obtain the same effect of reduction of strength as experimentally. The uprights tested and simulated range from short column (250 mm) to long column (2600 mm). The FE analysis includes material non-linearity and large displacements.*

1 INTRODUCTION

The aim of this paper is to analyse the influence of perforations on the behaviour of members subject to compression.

With this purpose some pieces of upright directly formed from the non perforated sheet were requested from a manufacturer. So perforations are the only different feature between the two series of specimens (Fig. 1).

Ten units of 4 m length (total 40 m) of each series: rack section (RS) and the same but non perforated section (NP) were supplied by the manufacturer. The profiles were cut at the following lengths (mm): 250, 400, 600, 800, 1000, 1200, 1500, 1800, 2200 and 2600 mm; 3 specimens each. Ten sets, of 3 specimens each, of different series have been tested and analysed.

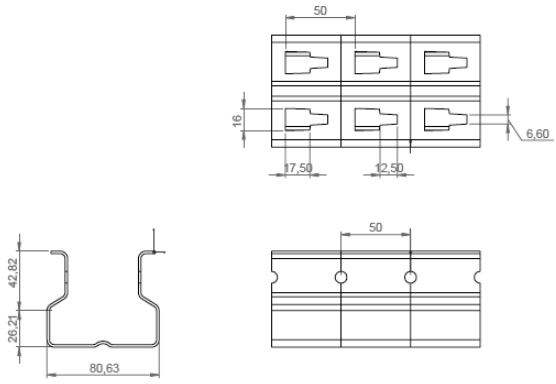

Main dimensions of the cross-section and perforations in the rack section (RS)

Figure 1: The uprights analysed.

Perforated cold-formed steel lipped C channel cross-sections have been analysed by Sputo & Tovar, and Moen & Schafer [1, 2, 3, 4].

Axially loaded, C-shaped cold-formed steel studs have been analysed [1, 2] by using the provisions of the Direct Strength Method (DSM). The Finite Strip Method (FSM) is used for determining the elastic buckling stresses. The buckling curve and buckled shapes are provided by CUFSM (Cornell University Finite Strip Method). To account for perforations three different models are developed: Solid web model, equivalent-thickness model and perforated model. Solid web model is the base model for analysis and is applicable to the calculation of local, distortional and longwave capacity. Mode interaction is analysed and discussed; and the capacities predicted using the DSM for the limit states of longwave, distortional and local buckling are compared to capacities calculated using the equations contained in the AISI Specification. This research concludes that the solid web model is the most appropriate model for determining longwave buckling strength, and the use of the equivalent thickness model is not recommended in longwave buckling. The results from this study predict higher local buckling strengths for the perforated model than the solid model.

Experimental tests and FE analysis on cold-formed steel lipped C channel columns with and without pre-punched slotted web holes have been carried out by Moen and Schafer [3]. Specimens have one slotted web hole at the mid-height of the short column (610 mm length), and two slotted web holes in the intermediate length columns (1219 mm). Eigenbuckling analysis is performed using ABAQUS. Buckled shapes (eigenmodes) and buckling loads (eigenvalues) for specimens with and without holes are compared. It is concluded that the presences of slotted holes cause a slight decrease in the ultimate compressive strength and have influence on the post-peak response and column ductility.

Simplified methods for approximating the critical elastic buckling loads of cold-formed steel members with holes have been developed and summarized by Moen and Schafer [4]. Approximations are verified using FE models with explicit holes. Global buckling of members with holes can be approximated using classical closed-formed analytic expressions by reducing cross-section properties. Distortional and local buckling are approximated using modifications to FSM.

An empirical method for the treatment of perforations in the Generalised Beam Theory (GBT) has been developed by Davies [5]. This method is applied onto uprights in pallet rack structures.

2 EXPERIMENTAL TESTING

Tensile test coupons were extracted from the sheet and tested to determining the actual strength of the material. The yield stress f_y is 423 MPa and the ultimate stress f_u is 491 MPa. Thickness is t= 1.83 mm.

The experimental set-up to test the upright specimens in compression has the following features (Fig. 2):

- At both ends of the specimen a special load plate is clamped. The plate is very stiff (carbon steel 30 mm thickness) and distributes the load uniformly over all the section. It is clamped to the section, fixing the web and the flanges with bolts and pads to distribute the pressure. It has been proofed that this special plate introduces in the end section of the specimen a local restraint, equivalent to the one introduced by welding the plate to the section [6].
- Both end plates are ball-pinned, but with torsional restraint. The ball position defines the force line. The relative position of the ball to the section can be changed by means of gauges, in steps of 0.5 mm, and so the optimal position of the force line (passing through the effective centre of gravity) can be found.
- With a previous set of test on stub columns (short columns), the position of the effective centre of gravity of the perforated (RS) and non perforated (NP) section has been determined.
- Force and displacement data have been recorded during tests.

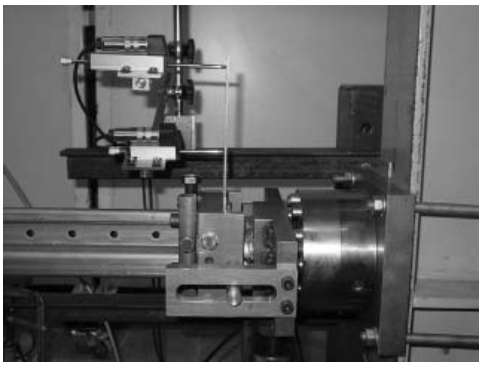

Figure 2: Experimental set-up.

The maximum loads obtained are summarized in Table 1.

Table 1: Experimental results (average of 3 specimens).

Length (mm)	$P_{ult,RS}$ (N)	Collapse mode	$P_{ult,NP}$ (N)	Collapse mode
250	144610	L	181160	L+(SD)
400	131913	SD	160143	SD
600	129305	SD	141357	SD
800	112097	SD	134200	SD
1000	109047	SD	131683	SD
1200	102797	SD(FT)	129940	AD+(FT)
1500	95670	AD+FT	113760	AD+FT
1800	75943	(AD)+FT	95613	(AD)+FT
2200	47597	FT	65710	FT
2600	44890	FT	50370	FT

L: Local. SD/AD: Symmetric/Asymmetric Distortional. FT: Flexural-Torsional

3 FINITE ELEMENT ANALYSIS

Numerical analyses are performed in such a way that experimental conditions are reproduced. The finite element model reproduces the actual section. In the Rack Section models (RS) the perforations are introduced with their actual geometry. Material is described by a multi-linear elastic-plastic model. The material properties are assumed to be constant over the section. Possible heterogeneities, anisotropy or residual stresses generated in the steel sheet during the forming process of the section are not known, and have not been introduced in the model.

The FEA is done in two stages:

- Stage I: Linear (eigenbuckling) analysis is carried out in order to obtain the eigen modes and select one of them to establish the initial geometric imperfections in the model to perform the non-linear analysis, and to obtain the critical load P_{crit}.
- Stage II: The selected mode is scaled to the maximum imperfection values, shown in Table 2, according to the buckling failure mode. With these initial displacements, a non-linear analysis is done, and the ultimate load P_{ult} is obtained.

Table 2: Imperfection values for non-linear analysis.

Mode	Magnitude	Reference
Local	Web/200	EN 1993-1-5:2006/AC:2009 [7]
Distortional	Flange/50	EN 1993-1-5:2006/AC:2009 [7]
Global	Length/1000	Commonly used in literature

Local and distortional imperfection magnitudes are taken from EC3 part 1.5 (plated structures), mostly used for welded plates, because there are none other in the code. However, these values are not too different from the usual ones available in the literature for cold-formed steel members [8]. For instance, local imperfection magnitude for the section studied is 0.4 mm versus 0.48 mm; and the distortional one is 1.38 mm versus 1.83 mm, respectively ([7] versus [8]).

Meshed sections (rack and non perforated section) are shown in Fig. 3.

Figure 3: Sections tested and analysed.

The maximum loads obtained are summarized in Table 3.

Table 3: FEA results.

Length (mm)	$P_{ult,RS}$ (N)	Collapse mode	$P_{ult,NP}$ (N)	Collapse mode
250	141942	L	174446	L+(DS)
400	126760	SD	150074	SD
600	122699	SD	142792	SD
800	112887	SD	130273	SD
1000	108490	SD	124811	SD
1200	106214	SD	121858	SD
1500	103805	(AD)+FT	113187	SD+(FT)
1800	84345	(AD)+FT	99048	FT
2200	61682	FT	71280	FT
2600	46302	FT	52880	FT

4 COMPARISON OF RESULTS

Next, in Fig. 4 and Fig. 5, maximum loads versus lengths of the member are depicted for both experimental and numerical tests. Results appear superposed in the graph and agreement can be seen.

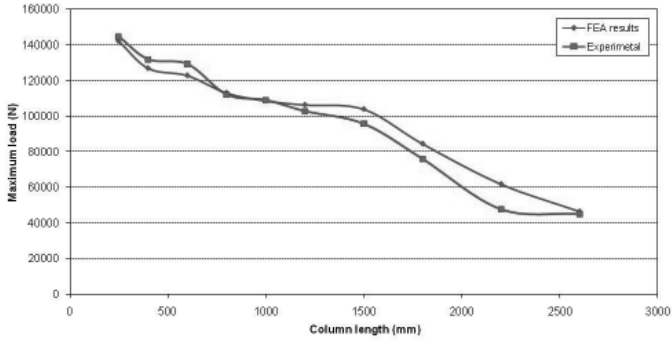

Figure 4: Maximum load versus length of the member (rack section).

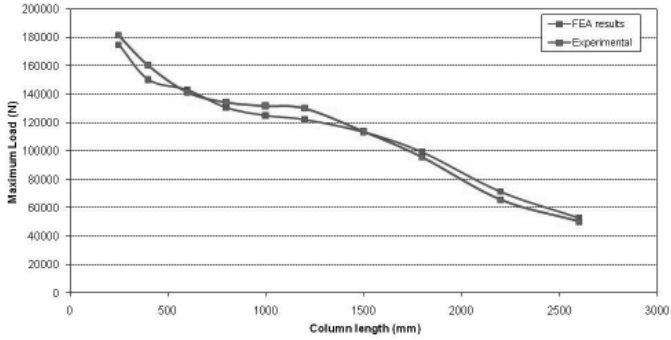

Figure 5: Maximum load versus length of the member (non perforated section).

The purpose of this paper is not to discuss the agreement or disagreement between experimental and numerical results, but attempting to give a procedure through which the critical and maximum loads of perforated sections can be determined from the non perforated section with an equivalent thickness.

5 EFFECTIVE OR EQUIVALENT THICKNESS

It is well known the equation for equivalent thickness given by Davies [5] based on the ratios of gross and net effective widths. A reduction factor for thickness presented by Salmi [9] and cited by Kesti [10], is determined from the elastic buckling stress of both perforated and non perforated plates.

The strategy followed herein has been to attempt to find the equivalent thickness by adjusting the critical load from linear analysis, which is very fast.

This equivalent thickness t_{eq} is applied to the whole section, and then the non-linear analysis either by FE analysis, or by any other method, can be done.

We define a reduction factor k: $t_{eq} = k \times t$, and a higher and lower bound for it:

$$k_{\text{sup}} = \frac{A_{RS}}{A_{NP}} \approx 0.93 \tag{1}$$

$$k_{\text{inf}} = \frac{A_{web,RS}}{A_{web,NP}} \approx 0.79 \tag{2}$$

$$t = 1.83 \text{ mm} \quad \Rightarrow \quad 1.45 \text{ mm} \le t_{eq} \le 1.7 \text{ mm} \tag{3}$$

where A_{RS}: area of specimen, with perforations; A_{NP}: area of specimen, without perforations; $A_{web,RS}$: area of the web of specimen, with perforations; $A_{web,NP}$: area of the web of specimen, without perforations.

So, for each length, equivalent thicknesses between 1.45 mm and 1.7 mm have been tried, and the one that gives a P_{crit} in the linear analysis -without perforations- closer to P_{crit} obtained with the real thickness -with perforations- is chosen. The results are summarized in Table 4.

Table 4: Equivalent thickness obtained by adjusting the critical load.

Specimen length (mm)	Rack section			Non perforated section			Difference (%)
	t (mm)	P_{crit} (N)	Critical mode	t_{eq} (mm)	P_{crit} (N)	Critical mode	
250	1.83	338162	L	1.67	339322	L	0.343
400	1.83	325603	L	1.68	326959	L	0.416
600	1.83	280425	SD	1.63	279527	SD	-0.320
800	1.83	229115	SD	1.63	231717	SD	1.136
1000	1.83	202291	AD	1.63	203463	AD	0.579
1200	1.83	173040	AD	1.63	175153	AD	1.221
1500	1.83	132506	AD+(FT)	1.63	132566	AD+(FT)	0.045
1800	1.83	100682	FT	1.61	100895	FT	0.122
2200	1.83	71634	FT	1.61	71464	FT	-0.237
2600	1.83	53182	FT	1.61	52788	FT	-0.741

Then, with these values of t_{eq} and the section without perforations (NP), the Stage II of the FEA (non-linear analysis) is repeated. The results are summarized in Table 5.

Table 5: Ultimate load obtained with a non-linear FE analysis, with non perforated section and t_{eq}.

Specimen length (mm)	Rack section			Non perforated section			Difference (%)
	t (mm)	P_{ult} (N)	Collapse mode	t_{eq} (mm)	P_{ult} (N)	Collapse mode	
250	1.83	141942	L	1.67	159562	L+(SD)	12,41
400	1.83	126760	SD	1.68	143093	SD	12.88
600	1.83	122699	SD	1.63	123476	SD	0.63
800	1.83	112887	SD	1.63	112117	SD	-0.68
1000	1.83	108490	SD	1.63	107758	SD	-0.67
1200	1.83	106214	SD	1.63	103458	SD	-2.59
1500	1.83	103805	(AD)+FT	1.61	108738	(AD)+FT	4.75
1800	1.83	84345	(AD)+FT	1.61	85551	FT	1.43
2200	1.83	61682	FT	1.61	61691	FT	0.01
2600	1.83	46302	FT	1.61	45944	FT	-0.77

It can be observed that the differences are very small for all specimen lengths, except for the two shortest: 250 and 400 mm. For these two lengths, with a (predominantly) local buckling mode, the t_{eq} obtained predicts an ultimate load excessively high.

An adjustment of t_{eq} for these two lengths by using the ultimate load values from the non-linear FE analysis gives a new value: $t'_{eq} = 1.46$ mm (far lower than the 1.67÷1.68 obtained with the P_{crit}).

In using this t'_{eq} value for 250 and 400 mm length, and the other t_{eq} values obtained before for the rest of lengths, the comparison of P_{ult} is done in the graph in Fig. 6. As it can be seen, the agreement is very good for all the lengths.

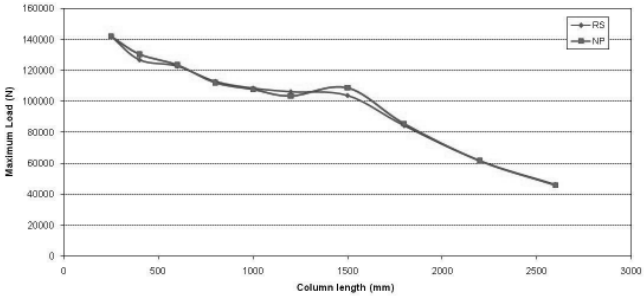

Figure 6: Maximum load versus length of the member (perforated and non perforated section).

So the procedure to find t_{eq} and t'_{eq} is schematized in Fig. 7.

6 CONCLUSIONS

- One upright design, with and without perforations, has been tested and analysed by FEA, under compression, with lengths from 250 to 2600 mm.
- The agreement between experimental and FEA results is good.
- An equivalent thickness t_{eq} is defined, to be applied to the non perforated section, with the aim of reproducing the same behaviour and the same results in the FE analysis as the perforated section with actual thickness t.

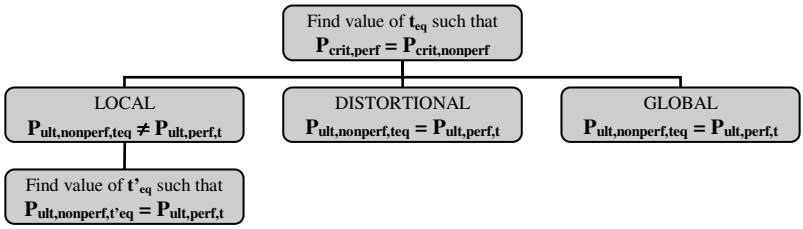

Figure 7: Procedure to find t_{eq} and t'_{eq}.

- This equivalent thickness is found by adjusting the thickness to obtain the same P_{crit} in the linear buckling analysis, which is very fast to do.
- The t_{eq} obtained can be easily classified into 3 groups (see Table 5):
  Group 1: Lengths 250 – 400 mm, t_{eq} = 1.67÷1.68 mm. In these columns the predominant failure mode is local buckling.
  Group 2: Lengths 600 – 1200 mm, t_{eq} = 1.63 mm. In these columns the predominant failure mode is distortional buckling.
  Group 3: Lengths 1500 – 2600 mm, t_{eq} = 1.61 mm. In these columns the predominant failure mode is global buckling.
- The equivalent thickness so obtained is used for the non-linear FE analysis. The results derived by comparing P_{ult} agree well for groups 2 and 3 (distortional and global buckling) (difference ≤ 4.75%), but do not agree well for group 1 (local buckling) (difference ≈ 12%).
- The agreement of P_{ult} derived with the t_{eq} proposed here is very good for columns that fail due to distortional and global buckling, but is not so good for short columns, where failure is predominantly local buckling.
- For group 1 (local buckling), a new equivalent thickness t'_{eq}, obtained by adjusting the P_{ult} in the non-linear FEA, is necessary to have a good agreement.
- The procedure proposed here to derive this t_{eq} by adjusting the P_{crit} through a linear FE analysis is very fast, and predicts very well the P_{ult} for columns failing in distortional and global mode.
- As only one upright section has been analyzed. To extend these conclusions to other sections, more experimental and simulation work is needed.

REFERENCES

[1] Sputo, T., Tovar, J. "Application of direct strength method to axially loaded perforated cold-formed steel studs: Longwave buckling", *Thin-Walled Structures*, **43** (2005), 1852-1881.
[2] Tovar, J., Sputo, T. "Application of direct strength method to axially loaded perforated cold-formed steel studs: Distortional and local buckling", *Thin-Walled Structures*, **43** (2005), 1882-1912.
[3] Moen, C., Schafer, B.W. "Experiments on cold-formed steel columns with holes", *Thin-Walled Structures*, **46** (2008), 1164-1182.
[4] Moen, C., Schafer, B.W. "Elastic buckling of cold-formed steel columns and beams with holes", *Engineering Structures*, **31** (2009), 2812-2824.
[5] Davies, J.M., Leach, P. and Taylor, A., "The Design of Perforated Cold-Formed Steel Sections Subject to Axial Load and Bending", *Thin-Walled Structures*, **29**(1-4), 141-157, 1997.
[6] Casafont, M., Roure, F., Pastor, M.M., Somalo, M.R. "Compression tests on uprights: Checks for the effects of distortional buckling", *2nd ERF Workshop "Tests on racking systems"*, Barcelona, Spain, 2010.
[7] *European Standard EN 1993-1-5:2006/AC:2009*. Eurocode 3 – Design of steel structures - Part 1-5: Plated structural elements. European Committee for standardization, Brussels, 2009.
[8] Schafer, B.W., Peköz, T. "Computational modeling of cold-formed steel: characterizing geometric imperfections and residual stresses", *Journal of Constructional Steel Research*, (**47**) (3), 193-210, 1998.
[9] Salmi, P., "Design of web-perforated steel wall studs" (In Finnish), *4th Finnish Steel Structures R&D Days*, Lappeenranta, Finland, 1998.
[10] Kesti, J., "Local and distortional buckling of perforated steel wall studs", *Dissertation*, Helsinki University of Technology, Espoo, Finland, 2000.